Efficient single-photon emission from electrically driven InP quantum dots epitaxially grown on Si(001)

M. Wiesner*, W.-M. Schulz, C. Kessler, M. Reischle, R. Roßbach,

M. Jetter, & P. Michler

Institut für Halbleiteroptik und Funktionelle Grenzflächen and Research Center SCoPE,

Universität Stuttgart, Allmandring 3,

70569 Stuttgart, Germany.

* *Email correspondence: m.wiesner@ihfg.uni-stuttgart.de*

The heteroepitaxy of III-V semiconductors on silicon is a promising approach for making silicon a photonic platform for on-chip optical interconnects[1–3] and quantum optical applications[4–6]. Monolithic integration of both material systems is a long-time challenge, since different material properties lead to high defect densities in the epitaxial layers. In recent years, nanostructures however have shown to be suitable for successfully realising light emitters on silicon[7–12], taking advantage of their geometry. Facet edges and sidewalls can minimise or eliminate the formation of dislocations[9], and due to the reduced contact area, nanostructures are little affected by dislocation networks[12]. Here we demonstrate the potential of indium phosphide quantum dots as efficient light emitters on CMOS-compatible silicon substrates, with luminescence characteristics comparable to mature devices realised on III-V substrates. For the first time, electrically driven single-photon emission on silicon is presented, meeting the wavelength range of silicon avalanche photo diodes' highest detection efficiency.

To date, numerous realisations of light emitting diodes (LEDs) or even lasers on silicon (Si) have been reported[13–15], mostly however using misoriented substrates or thick buffer layers, which precludes a direct integration in mainstream Si technology, as complementary metal oxide semiconductor (CMOS) processes require exactly oriented Si(001) substrates. Thick buffer layers cause large height differences and thus negatively impact high resolution lithography. Alternatively, III-V emitters have been realised on Si by hybrid technologies[16, 17], which however is a very complex method, making CMOS integration time-consuming and expensive.

The methods mentioned above are indispensable for providing optimal growth conditions required for spatially extensive layers, such as quantum wells. Defects within these layers deteriorate the optical and electrical characteristics of the device and may lead to reduced reliability. However, nanostructures were found to grow defect-free even in a sub-optimal environment[9] and thus represent an enclosed electronic system. Using quantum dots (QDs) as the active light emitting medium further provides the possibility to build up semiconductor lasers with superior performance, such as low thresholds and broader gain spectra. Over and above, self-assembled (QDs) are excellent candidates for single-photon sources, which are essential for quantum information science and technology[18–20].

Our self-assembled InP QDs were grown on exactly oriented Si(001) substrates by metal-organic vapour-phase epitaxy (MOVPE) using standard sources at low pressure in a horizontal reactor setup. QDs for photoluminescence (PL) measurements were deposited on a III-V buffer consisting of a strained $In_{0.06}Ga_{0.94}As$/GaAs superlattice between bulk GaAs layers, as shown in Figure 1a. The strain introduced by the supperlattice interacts with dislocations and suppresses propagation into overlying layers. Temperature cycle steps during buffer growth, performed in a range between 200°C and 790°C, further support dislocation reduction. QDs for electroluminescence (EL) experiments were grown on a more simplified buffer, solely consisting of a GaAs layer of 1 μm thickness. On top of each particular buffer, InP QDs were deposited, embedded in $(Al_{0.5}Ga_{0.5})_{0.51}In_{0.49}P$ and $(Al_{0.2}Ga_{0.8})_{0.51}In_{0.49}P$ layers serving as barrier material, lattice matched to GaAs.

For atomic force microscopy (AFM) investigations, QD structures were grown without capping layers. Figure 1b shows an AFM scan of a QD layer on top of the extended buffer structure. We mainly find lens-shaped structures of two different sizes. While the smaller ones are found all over the investigated area, the bigger ones are predominantly arranged in chains along the edges of trenches or valleys. This ordering phenomenon can be explained by effective local strain fields[21] at these locations leading to a preferred nucleation and assembling of InP. We will see later that the structures observed can be identified as two different types of QDs. By means of AFM analysis we can estimate the density of small QDs, in the following named 'type-A' QDs, to be $(4.2\pm1)\times10^{10}\,\mathrm{cm}^{-2}$ and for the large QDs ('type-B') we find $(1.9\pm1)\times10^{9}\,\mathrm{cm}^{-2}$.

The optical properties of the QDs were examined by investigations of the ensemble luminescence (see Methods). The temperature-dependent spectra are shown in Figure 2a. At 4.6 K, QD emission is observable as broad emission peaks around 1.70 eV (type-B) and 1.88 eV (type-A). At low temperatures, shallow localisation centres in the barrier material may trap the optically excited charge carriers. With increasing temperature these charge carriers can be thermally activated and so both types of QDs yield a higher intensity. A further increase in temperature then leads to a decreasing emission intensity, since charge carriers are thermally activated out of the QD and get lost for radiative recombination. Due to the stronger quantisation, this loss process is more severe for the smaller sized type-A QDs, having a smaller energetic distance between ground state and barrier. Type-B QDs have a smaller energy-level spacing and therefore more energy levels in the QD, which may

lead to a higher population number of carriers. In addition, carrier capture and relaxation processes are more efficient in type-B QDs, enabling luminescence up to 300 K. The emission characteristics and the quantum efficiency of the optically pumped QDs, as shown so far, are in good agreement with the findings for QDs grown on GaAs substrate[22].

The temperature-dependent ensemble luminescence from electrically pumped InP QDs grown on Si substrate is shown in Figure 2b. Again we see two types of QDs contributing to the emission at low temperatures, observable as two broad peaks at 1.73 eV and 1.91 eV. The slight shift of the peak positions compared to the optically pumped samples is caused by the doping of the structure, which causes a bending of the band structures due to the increased presence of free charge carriers. The emission of type-A QDs can be observed up to 80 K, and type-B QDs again show superior temperature stability even up to room temperature.

In order to confirm the correlation between the structures observed by AFM and the PL results, luminescence maps of the optically pumped QD sample were recorded (see Methods), as shown in Figure 3. The detected light was spectrally filtered, so that either the spectral range with dominant type-A (590 nm - 700 nm, Fig. 3b) or type-B (695 nm - 785 nm, Fig. 3c) QD emission could be investigated. Both maps show exactly the same section of the sample surface. Comparing these two figures, we clearly see different luminescence patterns for the different spectral ranges. The pattern originated by the long-wavelength luminescence centres (Fig. 3c) fits well to the distribution and dimension of trenches found by AFM investigations, and around which an agglomeration of large structures was found (Fig. 1b). The smaller-sized type-A QDs, which were found evenly spread all over the sample, emit in the spectral range detected in Figure 3b. In accordance with AFM results, centres of high luminescence were found evenly distributed throughout the investigated area.

Furthermore, samples were also subjected to μ-EL measurements (see Methods). Figure 4a depicts the emission characteristics of a single QD while varying the bias voltage. Starting at 2 V, we see a narrow line at 1.889 eV, which can be attributed to an excitonic transition, i.e. the recombination of an electron-hole pair. When more charge carriers are injected, it is getting more likely for a QD to capture further electrons and holes and form charged excitons or biexcitons. Increasing the voltage to 2.02 V, and thereby also increasing the injection current, an additional line emerges with an energy difference of 5 meV. This value fits well to the exciton-biexciton binding energy of approx. 4-6 meV in this material

system[23] and thereby indicates the zero-dimensionality of the light emitter. Figure 4b shows the temperature-dependent electrically pumped emission from a single QD. Luminescence can be observed up to 60 K, keeping up with electrically pumped InP QDs grown on GaAs substrates[24]. The electrical properties of structures realised on both types of substrates are as well in accordance, as apparent in Figure 4c. Here we see the diode characteristics of InP QD-based LEDs, on Si and GaAs, respectively. LEDs on Si show a low voltage drop and the same characteristics like mature LEDs in the GaAs material system.

Since light emitted by single QDs shows significant non-classical characteristics, second-order autocorrelation measurements $g^{(2)}(\tau)$ were performed in a Hanbury-Brown and Twiss-type setup[25] to further verify single dot emission[18]. The number of coincidence events versus the delay time τ is shown in Figure 5a and b for optically pumped QDs under pulsed excitation and in Figure 5c for an electrically pumped QD under DC current excitation. All measurements show a pronounced suppression of coincidences at $\tau = 0$. The QD in Fig. 5a reveals a $g^{(2)}(0)$ value of 0.08 at 4 K, which indicates a decrease in multiphoton emission events by a factor of approximately 12 when compared to a Poissonian source of the same average intensity. The deviation from $g^{(2)}(0)=0$, as would be expected for an ideal source, is caused by the limited temporal resolution of the experimental setup and by uncorrelated background emission. The latter is becoming more severe with increasing temperature, as apparent in the PL spectrum at 80 K (Fig. 5b). Nevertheless, autocorrelation measurements showed single-photon emission with $g^{(2)}(0) = 0.37$. Considering the contributions of the background emission[24], we obtained a corrected value for $g^{(2)}(0)$ of 0.15 at 80 K. Although measurements on optically pumped QDs were carried out under pulsed excitation, no correlation peaks can be identified at 4 K (Fig. 5a). This behaviour can be explained by charge traps in the barrier material, in which electrons and holes are stored after optical excitation. After the decay of the exciton in the QD, the charge carriers diffuse into the QD and thus populate it again before the next excitation pulse[26]. This refilling effect becomes less pronounced at higher temperatures, as the traps are then less populated. Consequently, at 80 K, correlation peaks are observable at multiples of the laser repetition rate (Fig. 5b).

The autocorrelation measurement on the electrically pumped QD, as displayed in Figure 5c, shows also non-classical characteristics, with a $g^{(2)}(0)$ value of 0.52. Here, background correction yields only a slight reduction down to $g^{(2)}(0) = 0.48$, which indicates that the temporal resolution of the measurement setup is probably the most constraining factor in

this case.

Since we did not deconvolute the instrument response function, all $g^{(2)}(0)$ values given here should be understood as an upper limit. With this first presentation of electrically driven single-photon emission on CMOS-compatible Si substrates, InP QDs have proven to be highly attractive light sources for future Si based photonic integrated circuits and quantum information technology.

Methods

For luminescence measurements, the samples were placed in a He-flow cold finger cryostat. A heater inside the cryostat enabled temperature control from 4 K to 300 K. We used a frequency-doubled Nd:YAG laser for optical excitation in continuous wave (cw) mode at 532 nm with a power density of 650 $\mathrm{Wcm^{-2}}$ on the sample. On samples with electrically pumped QDs, Cr/Zn/Au/Pt/Au-stripes were evaporated to form the p-contact, and an Al-layer deposited on the back of the sample provided the n-contact. A current source with a resolution of 0.1 mA was used for excitation. For μ-EL measurements, a 50× microscope objective collected the EL emission from an area in the order of a few $\mu\mathrm{m}^2$. Two stepper motors allowed horizontally and vertically moving the cryostat, with an effective spatial resolution of 50 nm in each direction. The density of optically active QDs was sufficiently low to investigate single dot emission without the need of shadow masks.

Recording of the luminescence maps was performed in a liquid helium bath cryostat. Illumination and detection of the sample was carried out through a 63× microscope objective, with the laser spot being moved by a galvo-scanner. A pinhole was placed in the detection light path in order to reduce the investigated area down to a spot size diameter of approx. 0.5 μm.

[1] The International Technology Roadmap for Semiconductors: http://www.itrs.net.

[2] Mathine, D. L. The integration of III-V optoelectronics with silicon circuitry. *IEEE J. Select. Topics Quantum Electron.* **3,** 952-959 (1997).

[3] Miller, D. A. B. Device requirements for optical interconnects to silicon chips. *Proc. IEEE* **97,** 1166-1185 (2009).

[4] Politi, A., Cryan, M. J., Rarity, J. G., Yu, S. & O'Brien, J. L. Silica-on-silicon waveguide quantum circuits. *Science* **320,** 646-649 (2008).

[5] O'Brien, J. L., Furusawa, A. & Vuckovic, J. Photonic quantum technologies. *Nature Photon.* **3,** 687-695 (2009).

[6] Almeida, V. R., Barrios, C. A., Panepucci, R. R. & Lipson, M. All-optical control of light on a silicon chip. *Nature* **431,** 1081-1084 (2004).

[7] Martensson, T. et al. Epitaxial III-V nanowires on silicon. *Nano Lett.* **4,** 1987-1990 (2004).

[8] Benyoucef, M. et al. Wavelength tunable triggered single-photon source from a single CdTe quantum dot on silicon substrate. *Nano Lett.* **9,** 304-307 (2009).

[9] Mi, Z. & Chang, Y.-L. III-V compound semiconductor nanostructures on silicon: Epitaxial growth, properties, and applications in light emitting diodes and lasers. *J. Nanophoton.* **3,** 031602 (2009).

[10] Tanoto, H. et al. Electroluminescence and structural characteristics of $InAs/In_{0.1}Ga_{0.9}As$ quantum dots grown on graded $Si_{1-x}Ge_x$/Si substrate. *Appl. Phys. Lett.* **95,** 141905-1 - 141905-3 (2009).

[11] Chen, R. et al. Nanolasers grown on silicon. *Nature Photon.* **5,** 170-175 (2011).

[12] Roest, A. L. et al. Position-controlled epitaxial III-V nanowires on silicon. *Nanotechnol.* **17,** S271-S275 (2006).

[13] Liang, D. & Bowers, J. E. Recent progress in lasers on silicon. *Nature Photon.* **4,** 511-517 (2010).

[14] Groenert, M. E. et al. Monolithic integration of room-temperature cw GaAs/AlGaAs lasers on Si substrates via relaxed graded GeSi buffer layers. *J. Appl. Phys.* **93,** 362-367 (2003).

[15] Kwon, O. et al. Monolithic integration of AlGaInP laser diodes on SiGe/Si substrates by molecular beam epitaxy. *J. Appl. Phys.* **100,** 013103-1 - 013103-7 (2006).

[16] Fang, A. W. et al. Electrically pumped hybrid AlGaInAs-silicon evanescent laser. *Optics Express* **14,** 9203-9210 (2006).

[17] Roelkens, G. et al. III-V/silicon photonics for on-chip and inter-chip optical interconnects. *Laser & Photon. Rev.* **4,** 751779 (2010).

[18] Michler, P. et al. A quantum dot single-photon turnstile device. *Science* **290,** 2282-2285 (2000).

[19] Yuan, Z. et al. Electrically driven single-photon source. *Science* **295,** 102-105 (2002).

[20] Santori, C., Fattal, D., Vuckovic, J., Solomon, G. C. & Yamamoto, Y. Indistinguishable

photons from a single-photon device. *Nature* **419,** 594-597 (2002).

[21] Ugur, A., Hatami, F., Schmidbauer, M., Hanke, M. & Masselink, W. T. Self-assembled chains of single layer InP/(In,Ga)P quantum dots on GaAs (001). *J. Appl. Phys.* **105,** 124308-1 - 124308-4 (2009).

[22] Schulz, W.-M. et al. Optical and structural properties of InP quantum dots embedded in $(Al_xGa_{1-x})_{0.51}In_{0.49}P$. *Phys. Rev. B.* **79,** 035329-1 - 035329-8 (2009).

[23] Beirne, G. J. et al. Electronic shell structure and carrier dynamics of high aspect ratio InP single quantum dots. *Phys. Rev. B.* **75,** 195302-1 - 195302-7 (2007).

[24] Reischle, M. et al. Electrically pumped single-photon emission in the visible spectral range up to 80 K. *Optics Express* **16,** 12771-12776 (2008).

[25] Hanbury-Brown, R. & Twiss, R. Q. *The Physics of Quantum Information Technology* (Springer, Berlin, 2000).

[26] Aichele, T., Zwiller, V., & Benson, O. Visible single-photon generation from semiconductor quantum dots. *New J. Phys.* **6,** 90 (2004).

Acknowledgements

The authors would like to thank E. Kohler for technical assistance with the MOVPE, A. Fuoss for sample preparation, M. Ubl for device processing, D. Richter for AFM measurements, J. Kettler for recording luminescence maps and T. Schwarzbäck for illustrative artwork.

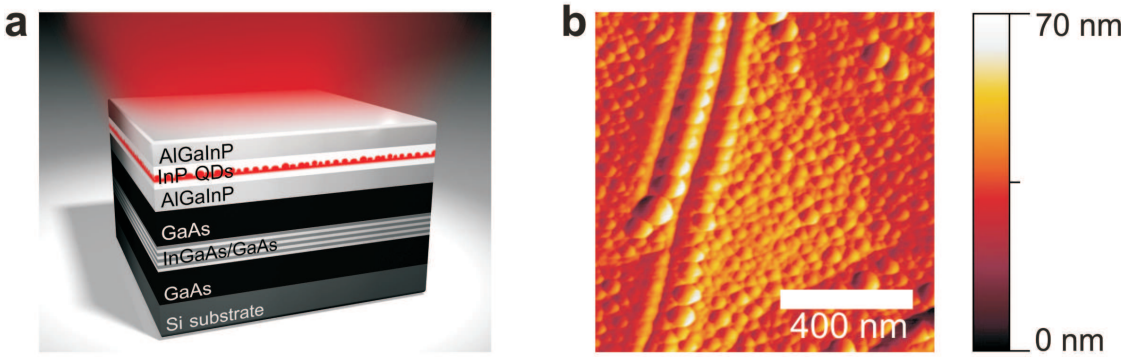

FIG. 1: **Sketch of the sample structure and AFM height measurement. a,** Optically pumped InP quantum dots were deposited on a buffer consisting of GaAs layers and a strained-layer superlattice of 10 periods $In_{0.06}Ga_{0.94}As/GaAs$. The superlattice thereby acts as a dislocation filter. AlGaInP-barriers enclose the QDs and provide effective charge carrier confinement. **b,** AFM image of a QD-layer grown on top of the same structure as depicted in (**a**), however without capping layers. The topology of the investigated section of a scale of $1\,\mu m^2$ exhibits an asperity with a difference in height of up to 70 nm.

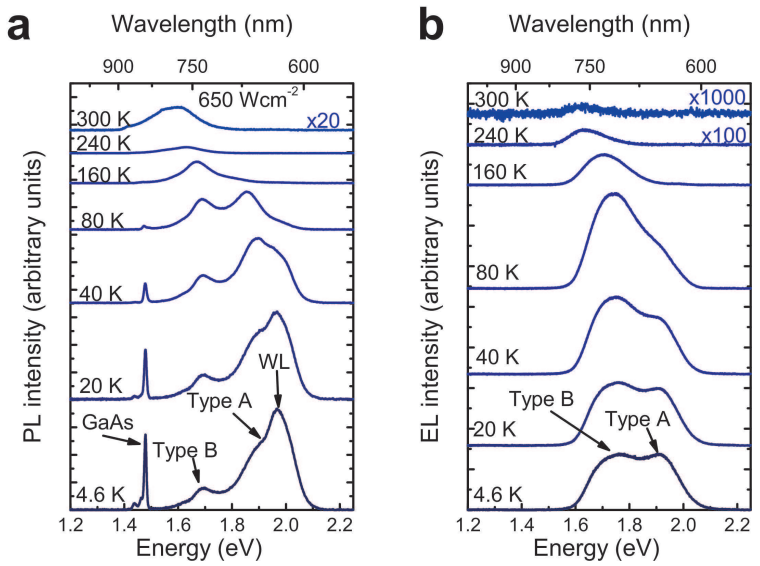

FIG. 2: **Temperature dependent ensemble luminescence. a,** Spectra of optically excited InP-QDs, showing the emission from the buffer (GaAs), wetting layer (WL) and two types of QDs (type A and B). **b,** Spectra of electrically pumped QDs, taken at a driving current of 50 mA with the applied voltage decreasing from 3.35 V at 4 K to 1.74 V at 300 K. Note that in the case of electrical excitation, neither WL nor GaAs luminescence is observable, as charge carriers are injected bidirectional and recombine mainly in the QD layer.

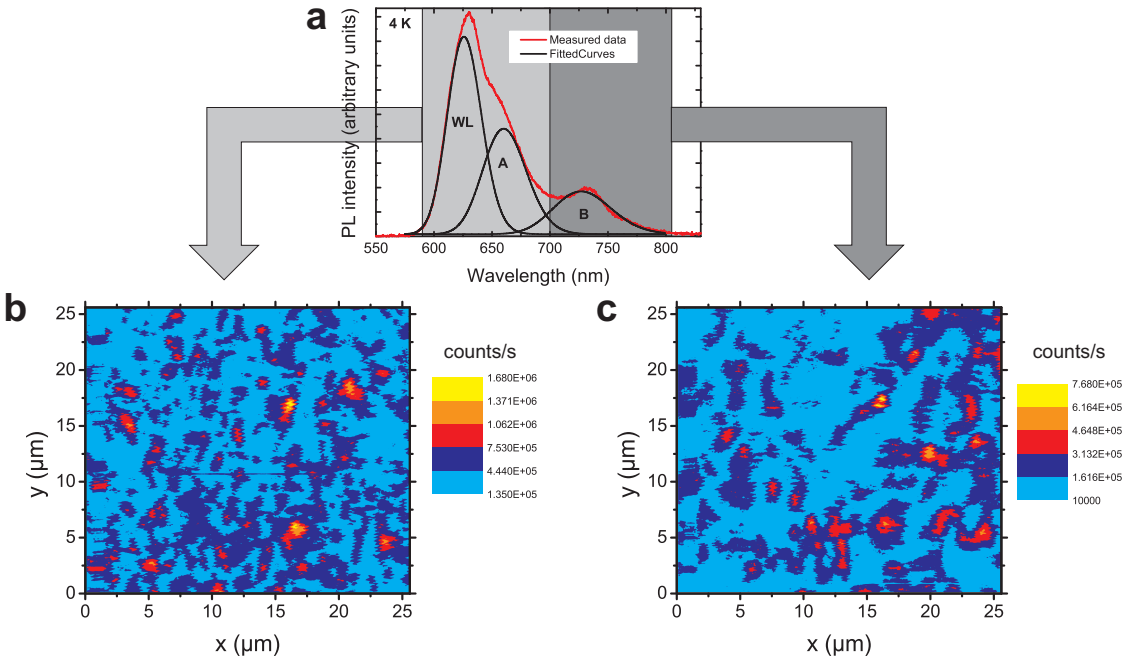

FIG. 3: **Spatial PL mapping. a,** Ensemble PL spectrum of the investigated sample at 4 K. The grey boxes illustrate the different spectral detection windows. Note that the emission from type A and B QDs partially overlaps and therefore can not be completely separated. **b and c,** PL maps showing the intensity (colour coded) for two different wavelength regions of the same surface section. Different colour scales were used for better visibility. We see different intensity patterns with apparently less light emitting centres in (**c**).

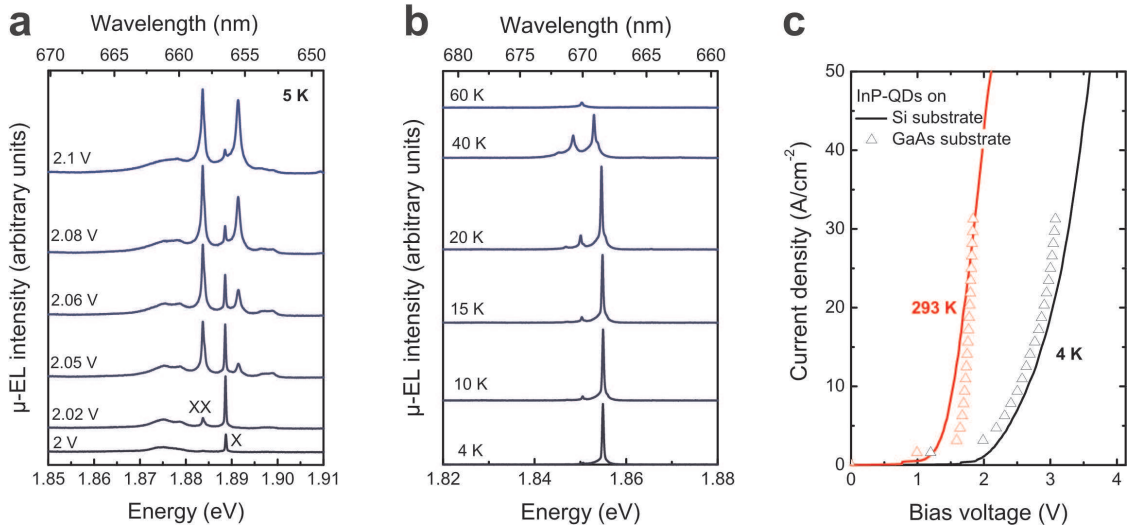

FIG. 4: **μ-EL measurements. a,** Emission from a single QD with increasing pump power. We can identify the emission of exciton (X) and biexciton (XX). Starting at an applied voltage of 2.05 V, an additional line emerges at 1.891 eV, which presumably originates from the emission of an adjacent high-energy QD or a charged exciton state. **b,** Temperature dependent EL from a single QD. All spectra were recorded at a bias voltage of 2.04 V. **c,** Diode characteristics of QD-based LEDs grown on Si (solid lines) and on GaAs substrates (symbols).

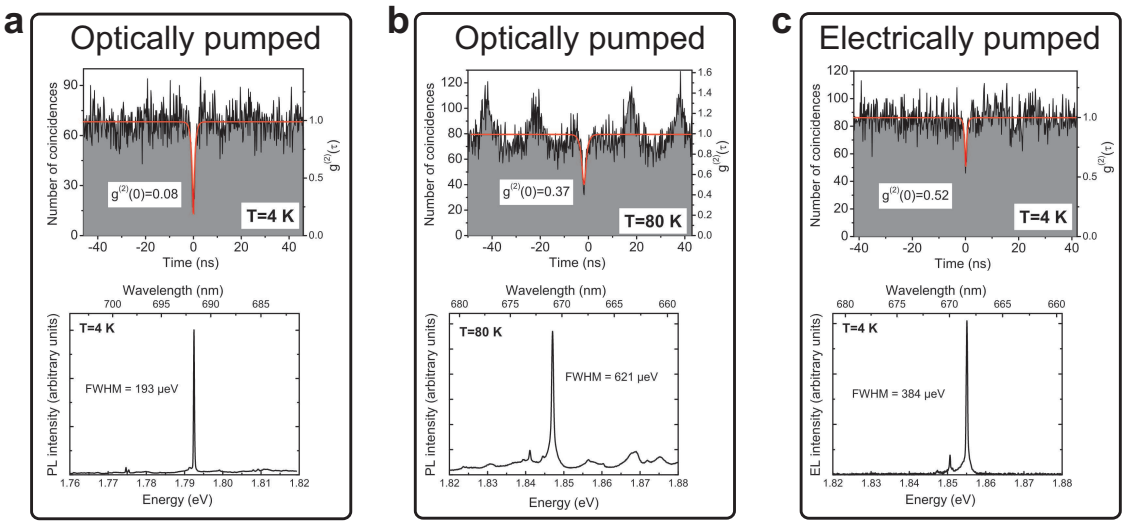

FIG. 5: **Second-order autocorrelation measurements.** No background correction or deconvolution of the instrument response function was applied. **a and b,** Measurements on optically pumped QDs under pulsed excitation at 4 K and 80 K, performed on the excitonic emission lines depicted underneath. Fast refilling processes, probably caused by charge traps, wash out the correlation peaks, which would be expected for pulsed excitation. At 80 K the charge traps are less populated, hence refilling effects decline. **c,** DC current autocorrelation measurements on the electrically pumped sample show a very narrow dip due to the limited temporal resolution of the measurement setup.